ResearchGate

See discussions, stats, and author profiles for this publication at: https://www.researchgate.net/publication/261325574

Energy-based thermal reflow simulation for 3D polymer shape prediction using Surface Evolver

Article *in* Journal of Micromechanics and Microengineering · April 2014

DOI: 10.1088/0960-1317/24/5/055010

CITATIONS
11

READS
322

3 authors:

Robert Kirchner
Technische Universität Dresden
39 PUBLICATIONS **212** CITATIONS
SEE PROFILE

Arne Schleunitz
Micro Resist GmbH
51 PUBLICATIONS **326** CITATIONS
SEE PROFILE

Helmut Schift
Paul Scherrer Institut (PSI)
167 PUBLICATIONS **3,024** CITATIONS
SEE PROFILE

Some of the authors of this publication are also working on these related projects:

MiFas - Microstructured Fiber Surfaces View project

X-ray Grating microfabrication View project

All content following this page was uploaded by Robert Kirchner on 16 July 2014.

The user has requested enhancement of the downloaded file.

IOP Publishing Journal of Micromechanics and Microengineering
J. Micromech. Microeng. **24** (2014) 055010 (7pp) doi:10.1088/0960-1317/24/5/055010

Energy-based thermal reflow simulation for 3D polymer shape prediction using Surface Evolver

R Kirchner[1], **A Schleunitz**[2] **and H Schift**[1]

[1] Paul Scherrer Institut, Laboratory for Micro- and Nanotechnology, 5232 Villigen PSI, Switzerland
[2] micro resist technology GmbH, Köpenicker Str. 325, D-12555 Berlin, Germany

E-mail: robert.kirchner@psi.ch and helmut.schift@psi.ch

Received 8 November 2013, revised 17 February 2014
Accepted for publication 24 February 2014
Published 3 April 2014

Abstract

An intensive, energy-based analysis of the thermal reflow of thermoplastic polymer structures is presented. Poly (methyl methacrylate) (PMMA) was patterned by grayscale electron beam lithography. The obtained rectangular, micron-scale structures were transformed into lens-like structures by thermal reflow near the glass transition temperature of the original PMMA. Representative parameters obtained from these reflow experiments were used to model the reflow process by using a new, energy-based, finite element, soapfilm method using the free software Surface Evolver. The time-, temperature- and molecular-weight-dependent geometry evolution of the PMMA structures could be described by an apparent contact-angle-evolution time constant and a shape-evolution time constant. The developed model allows the prediction of intermediate geometries during the reflow process occurring between the initial and the final energy optimal geometry. The proposed model is independent from the explicit knowledge of material-specific parameters such as viscosity or glass transition temperature. Extensive experimental data for PMMA reflow is provided. Simulation examples are given for a contact-angle-dominated reflow which demonstrate a good agreement between model and experiment.

Keywords: visco-elastic creep, topography equilibration, soapfilm, molecular weight, grayscale, electron-beam, nanoimprint

(Some figures may appear in colour only in the online journal)

1. Introduction

Polymer reflow has been used for micro-optics, especially micro-lens fabrication, for many years [1–3]. It has become a versatile method for three-dimensional (3D) pattern fabrication, which is in high demand, e.g., for future photonic and microfluidic device integration. Recently, an electron beam lithography and thermal reflow approach with topography equilibration was proposed to transform multi-step structures into continuous, smooth, wedge-like convex and concave structures [4, 5].

The thermal reflow process can be analytically described with hydrodynamic equations [6]. In particular, for aspherical microlenses without dynamic substrate wetting, an analytical, energy-based approach was proposed for geometry calculation [7]. While this is applicable for highly symmetric and periodic structures like microlens arrays, numerical models like finite element or volume methods [8] can be used for more complex structures. Elsewhere, such as in solder bump optimization, only the finally reflown, steady-state and minimal energy geometry is of interest. In such cases, purely geometrical considerations like truncated-sphere or force-balancing methods can be applied [9]. The dynamic wetting of polymers along a substrate can be described, for example, by a contact-angle wedge-flow [10] or an exponential decay [11].

This paper discusses an energy-based, finite-element, soapfilm approach to simulate the polymer geometry evolution

 © 2014 IOP Publishing Ltd Printed in the UK

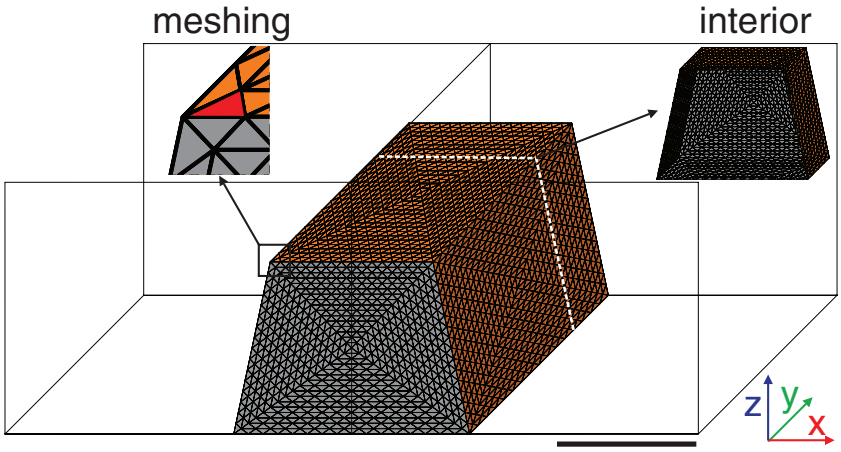

Figure 1. Meshed body geometry with insets showing the meshing by triangulation and the hollow body interior due to the soapfilm modeling for a 1700 nm wide line (scale bar 1 μm).

from initial structures toward an energetically optimized state including all intermediate geometries. This approach will allow an efficient full 3D computation of reflow structures for advanced micro- and nanofabrication. Exemplary structures were realized experimentally by stopping the evolution at a given point of time (a 'snapshot') and were then compared to simulated structures for verification.

An advantage of the soapfilm method is a reduced simulation effort due to there being fewer finite elements as compared to full 3D volume models. Thus, non-symmetric, complex structures can also be simulated in full 3D. The proposed model makes use of a parametrization from representative experiments. The freely available software circumvents problems associated with the proprietary simulation code and enables a straightforward adaption of the concept provided in this work to other reflow processes and alternative research fields.

2. Simulation model

2.1. Polymer reflow

Polymer reflow is a visco-elastic material behavior. It is viscosity and therewith time-temperature dependent. Similar to glass reflow [6], polymer reflow can be understood as a creep process, both on bulk surfaces and along interfaces. The polymer creep is driven by energetic imbalances which try to eliminate sharp corners and lead to polymer-substrate wetting. The smoothing is often exploited in photonics to yield low-loss waveguide sidewalls (e.g. [12]). The wetting is determined by the specific surface tension and surface free energy of the polymer melt and the substrate, respectively. A viscous polymer melt droplet will adopt a specific geometry on a substrate by interdependently optimizing: (i) the melt-substrate interface area and (ii) the melt surface area. During this optimization, the volume stays constant. The final droplet geometry represents the energetically optimal state within a given environment. For poly (methyl methacrylate) (PMMA) on native oxidized silicon, an energy optimal contact angle of roughly 22° can be estimated with the following equation

$$\alpha = \arccos\left(2\sqrt{\frac{\gamma_{SiO_2}}{\gamma_{PMMA}}} - 1\right) \qquad (1)$$

using a silicon oxide and PMMA surface energy of $\gamma_{SiO_2} = 30.7$ mJ m^{-2} [13] and $\gamma_{PMMA} = 33.1$ mJ m^{-2} [14] at 125 °C, respectively. However, this is only a rough estimation bearing the large variation of absolute surface energy values and the temperature influence in mind. Also, ideal PMMA wetting becomes easier with slightly higher substrate surface energies due to sample processing. The same physics are valid for polymer-reflow, i.e., the visco-elastic behavior. However, at temperatures close to the glass transition T_g there is significant rubber-elastic material behavior that is far away from a liquid flow region [15]. Creep with such elastic contributions can be explained using models containing Kelvin spring-dashpot elements [16]. In this model, the maximal polymer chain movement is limited by the spring being parallel to the dashpot.

The polymer reflow represents a dynamic transition from an initial (energetically not favorable) toward a final (energetically favorable) state. The speed of this transition is governed by time constants that are temperature and molecular-weight dependent.

2.2. Surface Evolver

Surface Evolver (SE) is a free simulation software that can determine optimum energy geometries for predefined energetic and geometrical constraints. SE was used to model microfluidic wetting geometries, which were then compared to experiments with a polymer melt as the example fluid [17]. A detailed description of the SE simulation principle is given in [18, 19]. SE is an energy-based tool which uses 2D finite elements to represent the surface of a full 3D model (figure 1). This is termed soapfilm modeling and requires a homogenous material to be used in approximations for the modeling of exposed PMMA regions.

Among the possible energies in SE, the most important is surface free energy or surface tension. Gravitational energy was neglected due to the micro-scale dimensions [17]. SE ascribes energies to 3D models as energy densities of the 2D finite elements. The total energy of the 3D model is then calculated from the model free surface and the interface areas. This overall energy is then reduced along an energy

gradient determined by iteratively moving the nodes of the finite element model by SE internal optimizing algorithms. Several optimization algorithms can therefore be chosen. For the model in this work, mean curvature flow (termed 'area normalization') was used for the surface-energy driven evolution. SE does not simulate dynamic liquid or polymer flow, it just calculates minimal energy geometries. However, this work proposes a method that uses its calculation engine to visualize the transition from the starting to the final optimal geometry. By doing so, all the intermediate states during the geometry evolution are accessible. To find the correct energy optimum, several customized simulation control routines are required (see next section).

2.3. Simulation control

The proposed model uses input parameters extracted from representative experiments. The model is thus independent from explicit material parameters. However, it can be applied to materials with known similarity. Those model parameters are different from typical material parameters such as viscosity, creep constants or material moduli. Such parameters require extensive rheological investigations and are often very difficult to obtain for typical electron beam resists like PMMA. In the case of PMMA that has been modified by electron beam exposure, those values are even more difficult to obtain as only small sample volumes can be provided. As well as the material properties, the surface properties (e.g. surface free energy) of the substrate are crucial for the reflow process. Parameters like the surface free energy are also very difficult to obtain for processed samples, e.g., electron-beam-exposed and developed ones. In contrast, the proposed concept uses parameters which can be well determined by standardized experiments, are very close to the realistic reflow process, and are appropriate for different geometries.

In this work, the simulation is controlled via two components: (i) apparent contact angle between polymer and substrate (contact-angle evolution); and (ii) change in total shape energy (shape evolution). The surface free energy γ_p of the polymer was assumed to be constant at a given temperature [14] and assigned to the free polymer surface (i.e. the triangular facets). With the apparent contact angle α obtained from SEM cross-sections of 100 μm long reflown single lines (cf figures 7(*a*) and (*b*)), the used model polymer-substrate interface energy γ_{ps} was calculated by

$$\begin{aligned} &\gamma_{ps} = \gamma_s - \gamma_p \cdot \cos(\alpha), \gamma_s := 0 \\ \Longrightarrow\ &\gamma_{ps} = -\gamma_p \cdot \cos(\alpha) \end{aligned} \tag{2}$$

and assigned to the model (i.e. the triangular facets). Equation (2) can be derived as a model from the Young equation. It uses a substrate surface energy $\gamma_s = 0$ to control the contact angle during simulation in a way that is consistent with SE conventions.

As mentioned above, the polymer creep is a dynamic process. Based on [11], α was expected to decrease exponentially with time for a given temperature and M_w. SE can optimize the interface and the free polymer surface, i.e., find the minimal energy geometry, based only on the input of this contact-angle–time relation. However, the reflow geometry at a certain point of time is not always the energy optimal geometry. For a correct prediction, a second control parameter, the shape evolution behavior, is required.

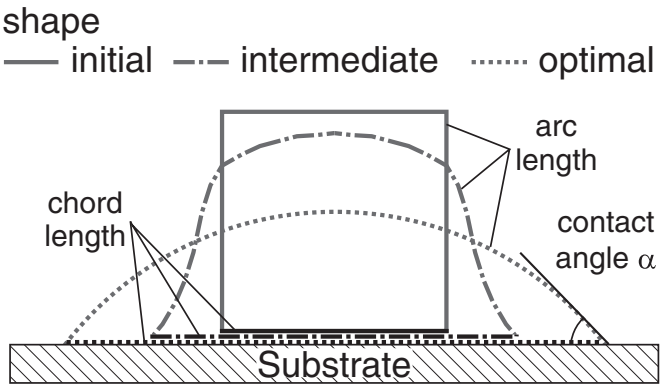

Figure 2. Schematic of shape evolution for an intermediate state and a final optimal state having the same contact angle α but highly differ from each other in shape and overall shape energy.

The shape evolution also depends on the polymer viscosity or mobility. In contrast to the contact-angle evolution, it is driven by the surface tension and local curvature of the polymer rather than the polymer surface tension and the substrate surface free energy. The contact-angle and shape evolution both depend on the M_w but occur on different time-scales. To have a measure of the ratio to which the shape already has approached its final state, we have defined a ratio R of the arc to the chord length of a shape for a given contact angle (figure 2).

The energy optimal shape has a constant curvature. Thus, the energy optimal ratio R_o can be calculated from a circle segment for any respective contact angle. The relative deviation r

$$r = \frac{R_c}{R_o} - 1 \tag{3}$$

of R_c at a given point of time to the optimal R_o defines the distance of a current shape to the optimal shape. The evolution of r toward the optimal shape was also assumed to be exponential.

The typical simulation steps comprised (i) geometry definition, (ii) boundary condition setting, (iii) parametrization, (iv) meshing by triangulation, (v) iterative evolution, consecutive data and geometry export as well as continuous mesh optimization to minimize mesh errors.

3. Experiment and simulation results

3.1. Sample preparation and methodology

Dose-modulated electron beam grayscale lithography [4] was used to write PMMA structures with different height levels (figure 3). The PMMA used was a nanoimprint resist provided by micro resist technologies GmbH (mr-I PMMA 120k). The main effect of the electron beam exposure (100 kV, Vistec EBPG 5000 Plus ES) was the reduction of the molecular weight M_w of the PMMA by chain scission [20, 21], which

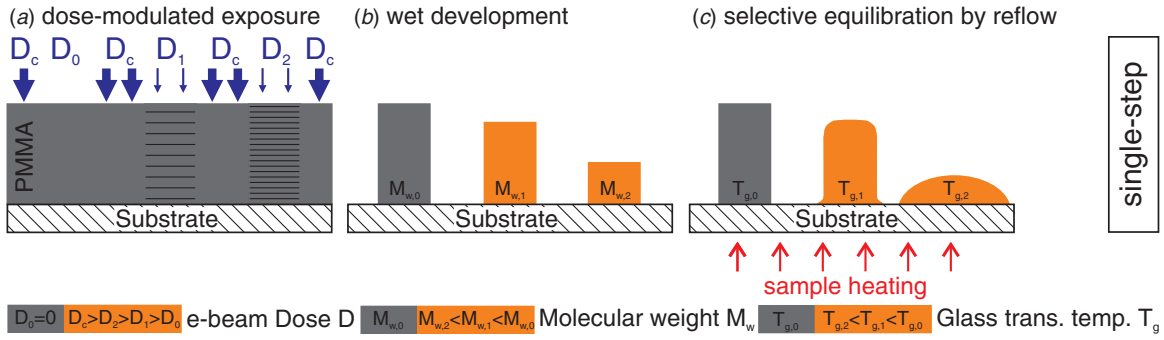

Figure 3. Schematic process flow used to obtain 3D reflow structures by (*a*) electron beam grayscale exposure, (*b*) development and (*c*) hotplate reflow. The used electron beam dose directly influenced the reflow behavior: while areas exposed with dose D_c were fully cleared, structures exposed with the lower doses D_1 and D_2 have a reduced height and a lower T_g in comparison to the unexposed structure (D_0) due to different molecular weights.

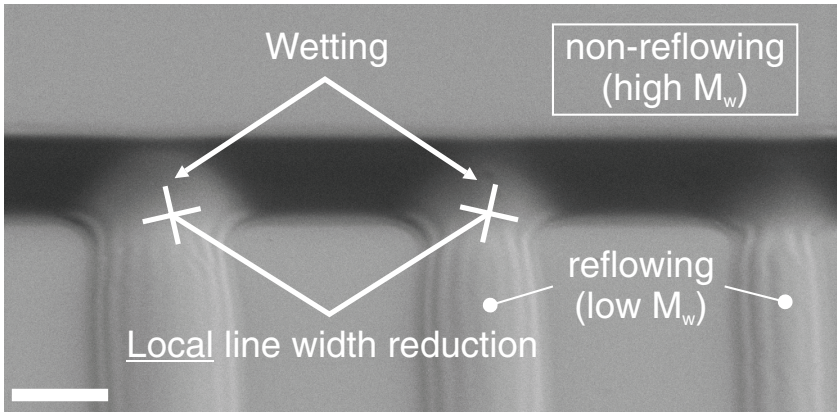

Figure 4. Scanning electron micrograph of the localized line width reduction at the end of 100 μm long lines after reflow due to wetting of the sidewalls, volume conservation and limited movement of the PMMA along the complete line length (scale bar 2 μm).

in turn increases the development rate in methyl isobutyl ketone and reduces the glass transition temperature T_g [5]. The reduced M_w increases the creep rate of the PMMA at a given temperature, as will be later shown in this work. Finally, the samples were heated on a hotplate for polymer reflow and immediately cooled down to room temperature after reflow. Scanning electron microscopy of cross-sections was used for geometry investigation. For improved understanding, the simulation method is discussed in this paper using single-step structures. Investigated line width ranged from 750 to 1800 nm.

In experiments, no significant influence of the line ends on the central part of the line was observed during reflow. The effect of sidewall-wetting at the line-ends on the line width was limited to the line ends (figure 4). Thus, the contact angle between the reflowing and non-reflowing polymer at the end of the polymer line was fixed at 90° for simulation and the length of the simulated line was not of importance.

3.2. Contact-angle evolution

The contact-angle behavior was highly temperature dependent and M_w specific, or in other words electron beam dose specific, as shown for exemplary 750 nm wide lines (figures 5 and 6). Because of rubber-elastic creep contributions and energy optimal final contact angles (cf section 2.1), a limited, asymptotic contact angle for long reflow times was found. Furthermore, the asymptotic contact angle decreased with higher temperatures and lower M_w due to weaker elastic contributions by shorter chains and a higher mobility. The experimental results in figures 5 and 6 were fitted to the following exponential equation together with the respective results for other line widths

$$\alpha\,(t) = \alpha_t = \alpha_\infty + \Delta\alpha \cdot \exp\left(-t/\tau_\alpha\right). \qquad (4)$$

By doing so, important parameters like the contact angle for infinitely long reflow times α_∞ as well as the time constant τ_α of the contact-angle evolution could be extracted. Please note that α_∞ is a practical fit obtained from experiments with a limited time-frame. While the contact-angle evolution of the unexposed material close to its $T_g \approx 120$ °C [5] occurred on the scale of the complete reflow experiment of 8 h (28,000 s), the reflow of the exposed structures was about up to one order of magnitude faster. Significant creep had already occured after 1 h (3,600 s) of reflow (table 1 τ_α). At lower reflow temperatures of 110 °C, creep of the exposed material was much slower.

3.3. Shape evolution

The shape optimization was determined by exponentially fitting the experimental decay of r over time toward the ideal

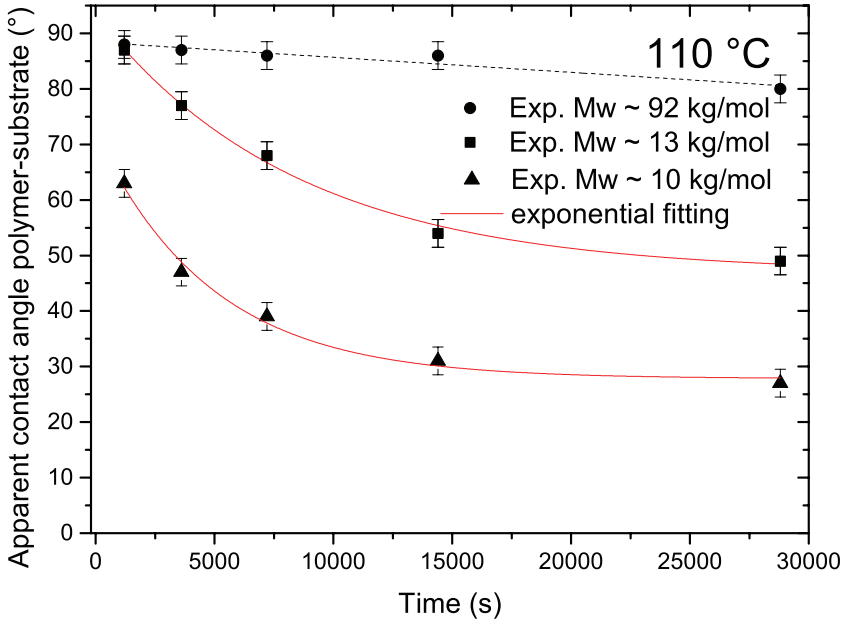

Figure 5. Evolution of the apparent contact angle α at a temperature of 110 °C, which is below T_g of the high molecular weight PMMA (circle, linear dashed line to guide the eyes) and at or above T_g of the low molecular weight PMMA (quadrat, triangle). Fit quality: $R^2_{\text{corr}} = 0.98...0.99$ and $\chi^2_{\text{red}} = 0.31...0.56$. Line width: 750 nm.

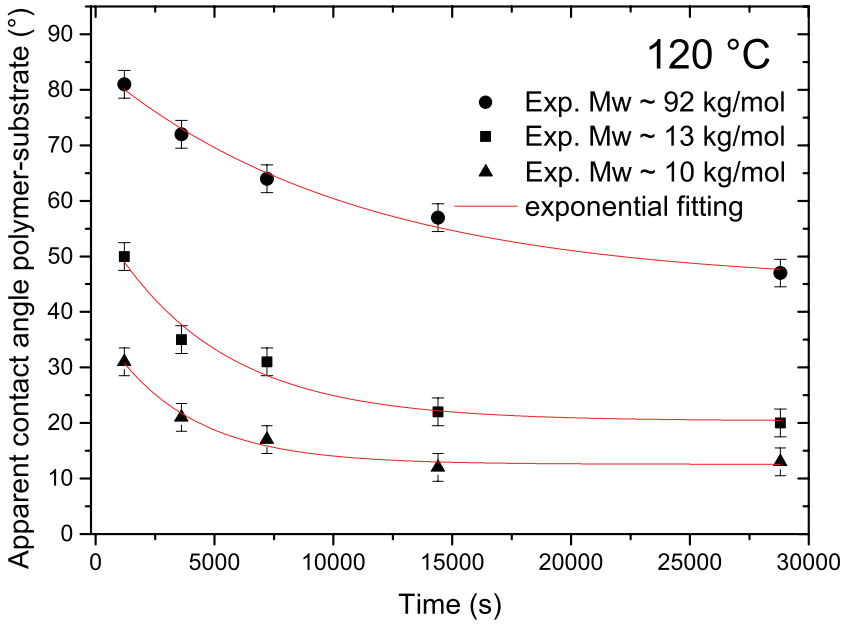

Figure 6. Evolution of the apparent contact angle α at a temperature of 120 °C, which is at or well above the T_g of all PMMA molecular weights (circle, quadrat, triangle). Fit quality: $R^2_{\text{corr}} = 0.95...0.98$ and $\chi^2_{\text{red}} = 0.25...0.37$. Line width: 750 nm.

Table 1. Experimental time constant ranges for contact-angle and shape evolution extracted with exponential models in equations (4) and (5) from several lines being between 750 and 1800 nm wide. (n.a.—not applicable because creep rate is much slower than experimental time-frame; []—low fitting quality; min. and max.—range for investigated feature size)

		110 °C		120 °C		110 °C		120 °C	
		τ_α (10^3 s)		τ_α (10^3 s)		τ_r (10^3 s)		τ_r (10^3 s)	
Effective dose (μC·cm^{-2})	M_w (kg·mol^{-1})	min.	max.	min.	max.	min.	max.	min.	max.
Unexposed	≈92	n.a.	n.a.	10.7	30.3	10.2	[112.1]	1.9	9.6
284	≈13	8.5	9.1	3.1	4.8	1.1	2.0	0.3	0.6
362	≈10	4.5	6.1	3.5	4.5	0.7	1.3	0.4	0.5

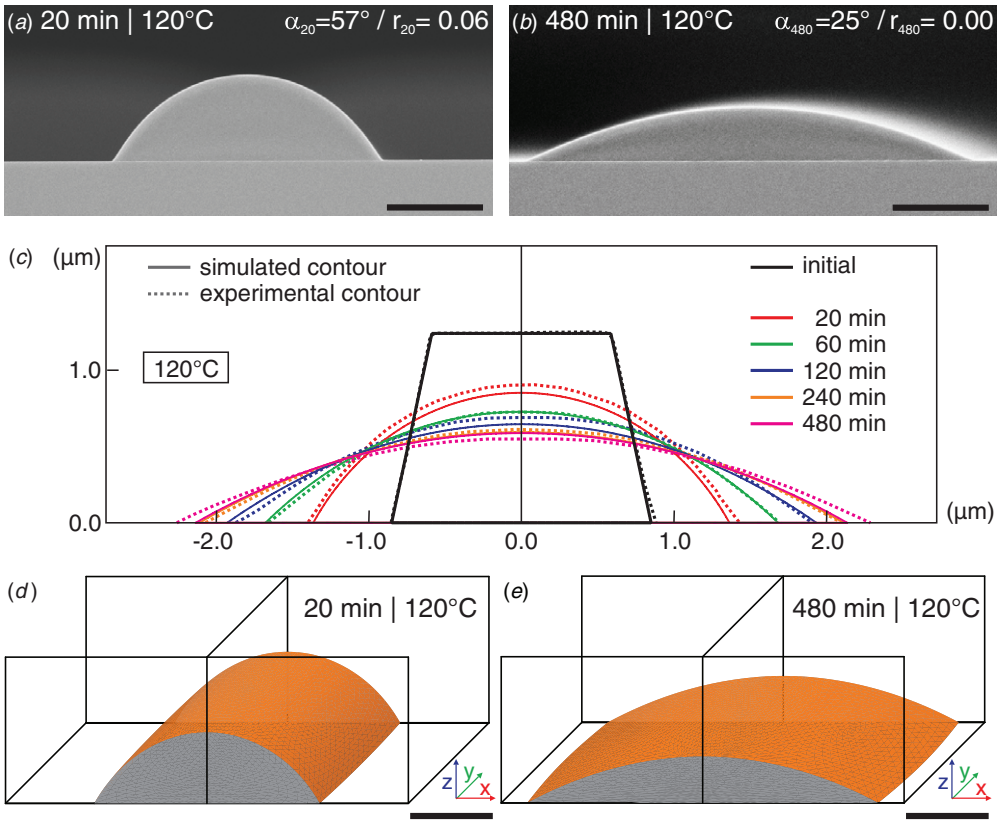

Figure 7. Comparison of (*a*) and (*b*) experimentally obtained scanning electron microscopy cross sections and (*c*)–(*e*) simulation of single 100 μm long and 1700 nm wide lines reflown for different times at a constant temperature (scale bar: 1 μm). (note: mesh in (*d*) and (*e*) disabled for better geometry visibility) (simulation parameters: $\alpha_\infty = 27\ ^\circ\text{C}$, $\Delta\alpha = 49\ ^\circ\text{C}$, $\tau_\alpha = 3108\ \text{s}^{-1}$).

shape ($r_\infty = 0$) using the following equation:

$$r(t) = r_t = r_\infty + \Delta r \cdot \exp(-t/\tau_r)\,,\ r_\infty := 0$$
$$\Longrightarrow r_t = \Delta r \cdot \exp(-t/\tau_r)\,. \tag{5}$$

The obtained fit was of high quality with R^2_{corr} values of 0.97 to 1.00 and 0.82 to 1.00 for the exposed and the unexposed material, respectively. Like the contact angles, the extracted values for the shape evolution were highly correlated with the electron beam dose and the respective M_w (table 1 τ_r). The extracted τ_α and τ_r values are representative for the M_w range and can be applied for simulation of geometries other than single lines. A clear trend for τ_r could be observed, with the minimum and maximum values in table 1 being always related to the smallest and largest line, respectively. For τ_α such a relation could not be found.

3.4. Model-experiment comparison

The contact angle α_t in equation (4) was used to control the wetting over time t via equation (2) in SE. The implementation of the shape evolution in equation (5) is the focus of ongoing research. Figure 7 shows a comparison of experimental and simulated reflow geometries ($M_w \approx 13$ kg mol^{-1}) for a contact-angle dominated reflow at 120 °C. The line width before reflow was 1700 nm. As can be seen from the scanning electron micrographs (figures 7(*a*) and (*b*)), after 20 min reflow an almost perfectly circular segment (constant curvature) is already present. This indicated a very fast evolution of the shape compared to the contact angle. This is also visible from table 1 for the observed time constants for $M_w \approx 13$ kg mol^{-1} material. For longer reflow times, almost optimal shapes with decreasing contact angles result from the reflow. There was a slight disagreement between simulation and experiment (figure 7(*c*)), especially for very long reflow times. This came from the fitting of the contact-angle evolution, which for the long reflow results in the slight difference between experimental (25°) and fitted contact angle (27°). Experimental variability was also responsible for the differences. Figures 7(*d*) and (*e*) show 3D surface representations of the simulated line for 20 and 480 min reflow at 120 °C having an almost constant curvature.

4. Discussion

A clear influence of time, temperature and molecular weight on the reflow process could be confirmed. This is characteristic of a visco-elastic polymer behavior. Regarding the variation in table 1, the influence of the line width is rather a challenge for the unexposed than the exposed material. We assume this variation to be related to the typical proximity effect during the electron beam exposure. Its effect on the M_w homogeneity is lower for grayscale features than for unexposed features.

For reflow at temperatures above the glass transition, the contact-angle evolution had a dominant influence on the

structure. Due to the much faster shape evolution compared to the contact-angle evolution of the system, the structure will always have an quasi optimal shape at any given contact angle. Two different contributions to reflow need to be considered. First, locally different Laplace pressures, originating from the polymer surface tension and locally different curvatures, which drive the shape evolution toward constant curvature geometries. Second, the contact-angle evolution, and thus the wetting of the polymer on the substrate, driven by the polymer surface tension and the substrate surface energy. Both contributions act simultaneously but on different time-scales, as discussed in this work. SE can calculate the shape evolution and its intermediate states for a constant contact angle. This was shown with an simulation example in [5]. There, the reflow was shape-evolution dominated, meaning a quick shape optimization with a constant contact angle due to the short time-frame of the experiment. This results in quasi-pinning at the polymer-substrate interface. As a consequence, multi-step structures are smoothed and undergo a process referred to as topography equilibration [5]. SE is not designed to simulate the dynamic polymer-substrate wetting. However, this behavior can be approximated for contact-angle dominated reflow behavior, as shown in this work. SE was used to calculate optimal geometries for time-discrete values obtained from equation (4).

Close to T_g, the speed at which the shape reaches its optimal energy for a given contact angle is comparable to the speed at which this contact angle evolves. For the simulation of reflow with such comparable contributions of the shape and the contact-angle evolution, a correlated computation of the two different time-scales in equations (4) and (5) would be required. This is the focus of ongoing work and thus not implemented in the current simulation model.

5. Conclusions and outlook

Extensive experimental investigations clearly indicated that thermoplastic polymer reflow is governed by the apparent contact angle and shape evolution. The presented energy-based simulation model allows the geometry prediction for contact-angle or shape-evolution dominated reflow separately. This enables the polymer reflow to be modeled beyond a pure shape optimization with quasi-pinning (constant contact angle). The model parametrization was done by efficient, direct measurement of the apparent contact-angle and shape evolution from the same set of electron micrographs. Thus, the simulation is independent from explicit knowledge of material specific parameters like viscosity or the glass transition temperature. Soapfilm modeling enables an efficient full 3D computation and will be useful, e.g., for a quick turn-around during nanoimprint master design and manufacturing.

Future work will address the combined shape-and-contact-angle based reflow close or at the glass transition temperature. The experiment-related, viscosity-independent model is therefore beneficial as reliable material parameters are difficult to obtain for the glass transition regime. Additional work will focus on a generalized relation between the structural evolutions and the molecular weight to minimize the experimental parametrization effort. The good agreement between experiment and simulation is very promising for future investigations, e.g., the simulation of multi-step structures.

Acknowledgments

The authors gratefully acknowledge micro resist technology GmbH for providing the PMMA as well as V Guzenko, C Padeste and K Vogelsang at PSI for their valuable support. The authors further express their thanks to H-C Scheer for valuable discussions.

References

[1] Ishihara Y and Tanigaki K 1983 *Proc. Int. Electron Devices Meeting* vol 29 pp 497–500
[2] Popovic Z D, Sprague R A and Connell G A N 1988 *Appl. Opt.* **27** 1281–4
[3] Heremans P, Genoe J, Kujik M, Vounckx R and Borghs G 1997 *IEEE Photon. Technol. Lett.* **9** 1367–9
[4] Schleunitz A and Schift H 2010 *J. Micromech. Microeng.* **20** 095002
[5] Schleunitz A, Guzenko V, Messerschmidt M, Atasoy H, Kirchner R and Schift H 2014 *Nano Convergence* **1** 1–7
[6] Chen Y, Yi A, Yao D, Klocke F and Pongs G 2008 *J. Micromech. Microeng.* **18** 055022
[7] Abe S and Sheridan J T 1999 *Phys. Lett.* A **253** 317–21
[8] Lee J-W, Feng Z, Engelstad R L and Lovell E G 2004 *Proc. SPIE* **5567** 1228–39
[9] Peng C-T, Liu C-M, Lin J-C, Cheng H-C and Chiang K-N 2004 *IEEE Trans on Components and Packaging Technologies* vol 27 pp 684–93
[10] Wei Y, Rame E, Walker L M and Garoff S 2009 *J. Phys.: Condens. Matter* **21** 464126
[11] Newman S 1968 *J. Colloid Interface Sci.* **26** 209–13
[12] Chao C-Y and Guo L J 2004 *IEEE Photon. Technol. Lett.* **16** 1498–500
[13] Thomas R R, Kaufman F B, Kirleis J T and Beisky R A 1996 *J. Electrochem. Soc.* **143** 643–8
[14] Wu S 1970 *J. Phys. Chem.* **74** 632–8
[15] Sperling L 2006 *Introduction to Physical Polymer Science* (New York: Wiley) pp 349–425
[16] Sperling L 2006 *Introduction to Physical Polymer Science* (New York: Wiley) pp 507–56
[17] Herminghaus S, Brinkmann M and Seemann R 2008 *Annu. Rev. Mater. Res.* **38** 101–21
[18] Brakke K A 1992 *Exp. Math.* **1** 141–65
[19] Brakke K A 2013 *Surface Evolver Manual V2.702013* www.susqu.edu/brakke/evolver/downloads/manual270.pdf
[20] Skinner J G, Groves T R, Novembre A, Pfeiffer H and Singh R 1997 *Handbook of Microlithography, Micromachining and Microfabrication* Vol 1 (Stevenage: SPIE) pp 380–476
[21] Dobisz E A, Brandow S L, Bass R and Mitterender J 2000 *J. Vac. Sci. Technol.* B **18** 107–11

View publication stats